Li-Ion Storage Models for Energy System Optimization: The Accuracy-Tractability Tradeoff

Fiodar Kazhamiaka*, Catherine Rosenberg*, Srinivasan Keshav*,
Karl-Heinz Pettinger†
University of Waterloo*, University of Applied Sciences Landshut†
{fkazhami}{cath}{keshav}@uwaterloo.ca, karl-heinz.pettinger@haw-landshut.de

ABSTRACT

There is a need for accurate analytical models that describe how a Lithium-ion battery's state of charge evolves as a result of a charging or discharging operation and that can be used in optimization problems. Although 'white box' models that take into account the details of electro-chemical processes can be highly accurate, they are not typically suitable for optimization problems. We propose two models that represent different tradeoffs between accuracy and tractability. We validate the accuracy of these models with data traces obtained from extensive experiments using two different commercially-available cells based on two distinct Li-ion technologies. We find that one of our models can be easily adopted for use in a mathematical optimization problem, while significantly increasing the range of C-rates over which it is accurate (<5% error) compared to the models that are currently being used.

CCS Concepts

•**Mathematics of computing** → **Convex optimization;**
•**Hardware** → **Batteries;**

Keywords

Li-Ion Storage; Modeling

1. INTRODUCTION

Although the cost of popular storage technologies, such as Lithium-ion (Li-ion) batteries, has been rapidly decreasing for the past decade, their cost continues to be a prohibitive barrier to adoption in applications such as electric vehicles and grid storage. Thus, there is a critical need to not only minimize the amount of storage needed for a given application but also operate it efficiently.

To fix ideas, one instance of a grid storage design application is to find the least storage needed to allow an inherently stochastic renewable generation process to meet a constant load; a classic optimization problem. Solving such a problem requires an *accurate* and *tractable* model for storage.

An ideal storage model should (a) allow us to accurately determine the energy content of the battery resulting from a series of charge or discharge operations and (b) be tractable, that is, be usable as part of an optimization problem. Specifically, the model should have the following characteristics:

1. It should be described using analytical, explicit expressions rather than, for example, a fixed point in a system of equations.

2. Its parameters should be easy to calibrate. Ideally, all parameters should be derived from the technical specifications of the battery, as published by the manufacturer.

3. It should be power-based, i.e., take power as input, rather than voltages and currents. This is because currents and voltage may vary in different parts of a battery system, but their product (excluding losses) is constant.

We note that there is an inherent tradeoff between accuracy and tractability: the more accurate the model, the less likely it is to be tractable. For an optimization problem it is desirable to use a *linear* model, as this guarantees the convexity of the problem and hence, the focus of this work is to develop a linear model.

If an ideal–accurate and tractable–model of storage existed, standard, powerful optimization techniques could study the operation and sizing of energy systems that incorporate storage, making them much more cost-effective than with *ad hoc* sizing and operation rules. Unfortunately, although some existing models are able to capture the behaviour of Li-ion batteries with high accuracy [7, 8], they do not satisfy one or more of the properties listed above.

In this work, we start from a well-known, simple and tractable model from the literature [6] and show that it fails to take into account some critical phenomena. We then propose a new model that takes these phenomena into account but is intractable and use it to derive a simpler linear model. We evaluate the accuracy of the two models we propose as well as of the original model from the literature on individual cells using measurements from two different Li-ion battery technologies and two cells for each technology. We use a methodology that allows us to separate modelling errors from parameter estimation errors. We show that the original model is accurate only in a narrow range of charging and discharging rates while our two models are more accu-

e-Energy'16, June 21–24, 2016, Waterloo, ON, Canada

DOI: http://dx.doi.org/10.1145/2934328.2934345

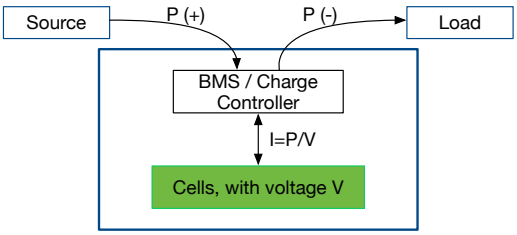

Figure 1: Battery system

rate and valid for a larger range of charging and discharging rates. Thus, our contributions are:

- Two new models for a Li-ion battery, one of which can be easily integrated into an optimization framework.
- A method to derive the model parameters from a manufacturer's specifications document.
- A thorough measurement campaign to validate our models as well as the simpler state of the art model on a single-cell battery by using a methodology that separates errors due to parameter estimation from model errors.
- Insights into the regimes in which the three models are accurate, depending on the properties of the Li-ion technology being modelled.

We give background information about Li-ion batteries and discuss existing literature in Section 2. We describe the state of the art and two novel models in Section 3, with an explanation of how to derive model parameters in Section 4. We present model validation in Section 5, discuss the results, insights, and modelling decisions in Section 6, and conclude the paper in Section 7.

2. BACKGROUND AND RELATED WORK

2.1 Lithium-ion Batteries

Li-ion batteries have seen a huge rise in popularity during the last decade. These batteries have many desirable properties, including high energy density, high efficiency, and fast charging/discharging capabilities. There are many variations in the chemical materials used in a Li-ion cell, and each variation results in a cell with different properties. For example, Li-Titanate cells have long life spans, while LiFePO4 cells can be discharged at very high power.

The price of Li-ion batteries is expected to continue to fall over the next 20 years [13], which bodes well for many applications where storage is a must or could be useful. Some key applications involve electric vehicles, grid regulation, and the integration of energy storage to allow solar and wind farms to provide power on demand rather than being limited by the variations in wind and sunlight.

2.2 Battery Components

A typical battery is composed of one or more cells and the associated battery management system (BMS). Figure 1 illustrates the battery. Power from a generator flows to the BMS, which charges the cells at a particular charge current; the product of the cell voltage and the charge current is the injected power. Symmetrically, the product of the cell voltage and the discharge current is the power drained from the cell, and available from the BMS. In this paper, we assume that the BMS is 100% efficient. The BMS confines the voltage of the cell to a range of acceptable values in order to avoid damaging it. We will refer to the endpoints of the voltage range as V_{min} and V_{max}. The BMS protects the cells from being damaged through over/undercharging by preventing any charging or discharging when the voltage is at V_{max} or V_{min}, respectively. The BMS also prevents cell damage at high power by clipping the power so that it stays in the allowed range.

2.3 Charging Behaviour

Several approaches for charging a Li-ion battery are known [20]. The most widely used protocol is referred to as Constant Current - Constant Voltage (CC-CV) charging. To understand this approach, it is first necessary to understand the behaviour of battery during charging and discharging.

When the battery is idle, its voltage is a good indicator of the amount of energy it contains. An idle voltage equal to V_{max} indicates that the battery is fully charged. However, when a charging current is applied, the battery voltage instantaneously jumps, only to fall back down when charging is stopped. The magnitude of the voltage jump (or drop) is approximately proportional to the current. Similarly, there is a voltage drop during discharging that is roughly proportional to the magnitude of the discharging current.

To prevent the battery voltage from exceeding V_{max} during the charging process, when the battery's energy content is high, the charging current is limited. Thus, the CC phase first charges the battery at a high current until it is nearly full, which causes the voltage to reach the upper limit. Subsequently, the CV phase reduces the current while maintaining the voltage at the upper limit.

In this paper, we show that it is important for a Li-ion battery model to take the voltage 'jump' and 'drop' into account. Specifically, we show that it is necessary to properly limit the charging current so that voltage limits are followed and to accurately estimate the change in the state of charge of the battery after each charging or discharging operation.

2.4 Existing Models

There is a rich and growing corpus of work on the topic of modelling energy storage. The most sophisticated models are based on modelling the internal chemical state of the battery [17], or modelling the battery as an equivalent electrical circuit [7, 8]. These models are able to estimate battery energy content and voltage, but at the cost of narrowing the scope of their application. More precisely:

1. Circuit-based models require current as input, and this current must be correctly estimated, which is challenging in practice.
2. It is difficult to estimate model parameters from the manufacturer's specification sheet. For example, Reference [7] uses genetic algorithms to identify certain model parameters, and the comparison of 12 equivalent circuit models in Reference [8] relies on multi-swarm particle optimization to find the best choice of model parameters.
3. The mathematical description of these models is complex. This presents a challenge if these models are to

be used as part of a simulation or mathematical optimization framework.

Thus, in work where a storage model is incorporated into an optimization problem, such as in References [2, 4, 5, 9, 10, 12, 15], the model is reduced to a simple set of linear equations and constraints. A typical version of this model, henceforth referred to as Model 1, is described in [6] and in Section 2.5. The simplicity of this model is gained at the cost of accuracy, as discussed next.

Note that this model can be used to derive an optimal operating strategy [10] or for sizing. In the first case, the parameters of the battery can be obtained using the battery specification sheet as discussed later. If it is used for sizing, the parameters of the battery have to be scaled appropriately. In this paper, we do not consider this problem of scaling, i.e., we model a given Li-ion battery assuming we have its specifications sheet.

2.5 Model 1

Model 1 incorporates several real-world aspects: limits on the energy content, maximum charge/discharge powers, and self-discharge. It models the limits on the energy content, with a_1 defined as the lower limit, $a_1 \geq 0$, and a_2 as the upper limit, where $a_2 \leq 1$. Limiting the energy content is often done in practice to avoid the increased wear on the storage that occurs when the cell energy content is at upper or lower extremes of the storage capacity, thereby increasing the lifetime of the storage. Model 1 also has limits on the maximum charging and discharging rates (powers), defined as α_c and α_d, respectively. Self-discharge is modeled using two parameters, with γ_1 being the fraction of energy content ($b(k)$) that is lost every time unit and γ_2 being the constant power drain. A description of each variable and parameter can be found in Table 1.

Model 1 is described using the following set of equations and constraints:

$$b(k) = (1-\gamma_1)b(k-1) + \Delta_E(k) - \gamma_2 T_u \quad (1)$$

$$\Delta_E(k) = \begin{cases} \eta_c p(k) T_u & : p(k) \geq 0 \\ \frac{p(k)}{\eta_d} T_u & : p(k) < 0 \end{cases} \quad (2)$$

$$\alpha_d \leq p(k) \leq \alpha_c \quad (3)$$

$$a_1 \leq b(k) \leq a_2 \quad (4)$$

where $b(k-1)$ is the energy content in the previous time step, and $\Delta_E(k)$ is an internal variable representing the change in energy content as a result of the applied power $p(k)$. It is a power model, meaning that it does not represent voltages or currents. When we validate Model 1 in Section 5 on individual cells, we notice some clear deviations between the model and the behaviour of a real cell. These deviations are caused primarily by two physical phenomena that are not taken into account in Model 1.

1. Model 1 does *not* reflect the well-known physical phenomenon that the battery's energy capacity changes with the charge or discharge current being applied. This behaviour, observed in Li-ion batteries [14], is similar to Peukert's Law for Lead-Acid batteries.

2. Model 1 treats both the charging and discharging efficiencies as constants, whereas in reality they depend on the magnitude of the current (see Section 4.4 for details).

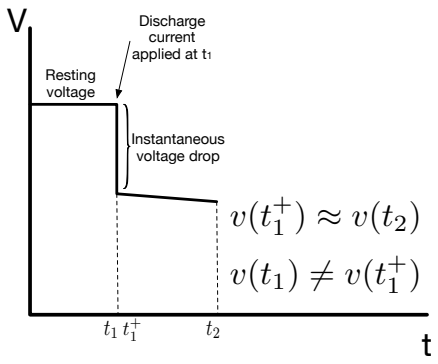

Figure 2: The battery voltage has a near-instantaneous drop when there is a change in the charging or discharging current. Here we illustrate a voltage drop when an increased discharging current is applied to the battery.

We use Model 1 as a starting point for developing more sophisticated models that take these effects into account.

3. MODEL DESCRIPTIONS

Table 1: Notation

Name	*Description (units)*
Battery parameters	
a_1	Minimum energy content (Wh)
a_2	Maximum energy content (Wh)
$\alpha_c(\alpha_d)$	Charge (discharge) rate limits (W)
$\eta_c(\eta_d)$	Charge (discharge) efficiency. Both are ≤ 1
γ_1	Leakage rate per time unit as a fraction of state of charge
γ_2	Constant leakage rate (W)
Model parameters	
U	Energy content at $k = 1$ (Wh)
T_u	Length of time slot (hours)
Model input	
$p(k)$	Power used to charge (discharge, if negative) the battery in time slot k (W)
Model variables	
$b(k)$	Energy content of the battery in time slot k (Wh)
$V(k)$	Voltage of the battery in time slot k (V) (only Model 2)
$I(k)$	Charge/discharge current (A)

This section will describe how we model time, followed by the description of our two models that use Model 1 as a starting point. Model 2 improves on Model 1 and is the most complex. Model 1* uses approximations to the improvements made in Model 2 to make it linear.

We express our models as a series of equations and constraints that together describe the effect of a single charge or discharge operation, within the feasible operating range of the battery. As with Model 1, our models are Markovian, and use the energy content of the previous time step and the applied power to calculate the present energy content. Model 2 also uses the voltage of the previous time step as an input.

3.1 Time

We treat time as having discrete slots, with time slots of

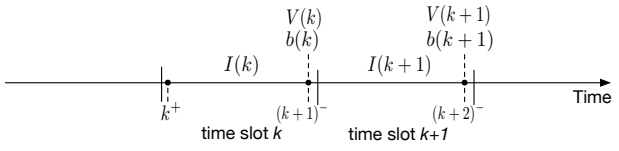

Figure 3: Illustration of time slots.

length T_u. For modelling purposes, it is tempting to make the assumption that all variables, such as voltage $V(k)$, current $I(k)$, and energy content $b(k)$, are constant within one time slot, with changes occurring only at the beginning of time slots. In practice, however, this assumption can introduce errors into the way we calculate the power flowing in or out of the battery in each time slot. For example, if we increase the discharging rate significantly at the beginning of a time slot, the voltage of a battery has been observed to drop almost instantly. Figure 2 illustrates this occurrence, which makes it clear that to calculate the power used to charge the battery or drawn from the battery in time slot k, it is more accurate to use the voltage at the end of the time slot rather than at the beginning. For this reason, we assume that the voltage is constant in the interval $[k^+, (k+1)^-]$, and use the voltage at the end of time slot k. Thus, we define $I(k)$ to be the current during time slot k, and $b(k)$ and $V(k)$ as the respective energy content and voltage at the end of the time slot. This notation is illustrated in the diagram shown in Figure 3.

3.2 Model 2

In Model 2, we extend Model 1 to use current ($I(k)$) and voltage ($V(k)$) as (internal) model variables[1]. We replace the contant a_1 (upper) and a_2 (lower) limits on energy content with functions that depend on the current, denoted $a_1(I)$ and $a_2(I)$. We also replace constant efficiency parameters η_c and η_d with functions, denoted as $\eta_c(I)$ and $\eta_d(I)$ for charging and discharging efficiency, respectively.

The following set of equations and constraints describes Model 2:

$$b(k) = (1-\gamma_1)b(k-1) + \Delta_E(k) - \gamma_2 T_u \quad (5)$$

$$\Delta_E(k) = \begin{cases} \eta_c(I(k))p(k)T_u & : p(k) \geq 0 \\ \frac{p(k)}{\eta_d(I(k))}T_u & : p(k) < 0 \end{cases} \quad (6)$$

$$V(k) = V(k)^* \quad (7)$$

$$I(K) = \frac{p(k)}{V(k)} \quad (8)$$

$$\alpha_d \leq p(k) \leq \alpha_c \quad (9)$$

$$a_1(I(k)) \leq b(k) \leq a_2(I(k)) \quad (10)$$

The inputs to the model are the parameters (γ_1, γ_2, $\eta_c(I)$, $\eta_d(I)$, α_c, α_d, $a_1(I)$, $a_2(I)$), the empirically-derived function M (described below), as well as the previous energy content $b(k-1)$, previous voltage $V(k-1)$, and input power $p(k)$. The output of the model is the battery energy content $b(k)$. $V(k)^*$ is an internal variable that is a fixed point of the iterative process described next.

We first estimate the voltage in time slot k using a predicted energy content and the input power. Let M be a function that maps the energy content and current to the cell voltage:

$$V(k) = M(b(k), I(k)) \quad (11)$$

M can be empirically derived from the reversible capacity curves obtained from the battery specifications (see Section 4.3 for details). However, this function alone does not allow us to predict the voltage. Specifically, although the change in energy level $b(k)$ can be obtained from Eq. 5, it is dependent on $I(k)$, which can be calculated from the following equation:

$$I(k) = \frac{p(k)}{V(k)}. \quad (12)$$

If we follow these calculations, a loop emerges: we need $b(k)$ to calculate $V(k)$, need $I(k)$ to calculate $b(k)$, and need $V(k)$ to calculate $I(k)$. To get around this, we introduce three new variables $\hat{V}(k)$, $\hat{I}(k)$, and $\hat{b}(k)$ that are the estimates for $V(k)$, $I(k)$, and $b(k)$. Given the input $p(k)$, we compute these estimates using the following iterative process, using the most recent estimates $\hat{V}(k)$, $\hat{I}(k)$, and $\hat{b}(k)$ in each step:

Step 1: Initiate $\hat{V}(k)$ as $V(k-1)$

Step 2: Calculate $\hat{I}(k)$ using Eq. 12

Step 3: Calculate $\hat{b}(k)$ using Eq. 5

Step 4: Calculate $\hat{V}(k)$ using Eq. 11

Step 5: Repeat Steps 2, 3, and 4 until $\hat{V}(k)$ converges to a fixed point $V(k)^*$.

In the thousands of cases where we have used this process, it has converged quite quickly, usually within a few iterations. The convergence takes only a handful of iterations when the initial value is close to the fixed point, which is why we take the voltage of the previous time slot as an initial guess to decrease the number of iterations.

Since M is defined only for voltages in the permitted range $[V_{min}, V_{max}]$, the voltage limits are implicit in M.

Model 2 covers the noticeable shortcomings of Model 1, but at the cost of increased complexity. The η_d, η_c, a_1, and a_2 functions may not be linear, and the iterative computation that implicitly defines $V(k)^*$ makes it difficult to integrate this model as part of a larger optimization model.

3.3 Model 1*

Model 1* is a simplified version of Model 2. It uses linear approximations to the implicit and non-linear parts of Model 2, specifically the recursive voltage estimation, efficiency functions, and energy limit functions:

- We approximate the voltage with the nominal voltage. The nominal voltage is different for charging and discharging i.e., $V(k) = V_{nom,c}$ or $V_{nom,d}, \forall k$, hence the charging current is approximated as $p(k)/V_{nom,c}$ and discharging current as $p(k)/V_{nom,d}$.
- The efficiency functions, $\eta_c(I)$ and $\eta_d(I)$, are replaced with constants, as is done in Model 1.
- The energy limit functions, $a_1(I)$ and $a_2(I)$, are replaced with linear approximations and become functions of $p(k)$.

[1]Note that Model 2 is still a power-based model.

These approximations trade off accuracy for tractability. A further discussion on these approximations can be found in Section 6.2.

The following set of equations and constraints describes Model 1*:

$$b(k) = (1-\gamma_1)b(k-1) + \Delta_E(k) - \gamma_2 T_u \quad (13)$$

$$\Delta_E(k) = \begin{cases} \eta_c p(k) T_u & : p(k) \geq 0 \\ \frac{p(k)}{eta_d} T_u & : p(k) < 0 \end{cases} \quad (14)$$

$$\alpha_d \leq p(k) \leq \alpha_c \quad (15)$$

$$a_1(\frac{p(k)}{V_{nom,d}}) \leq b(k) \leq a_2(\frac{p(k)}{V_{nom,c}}) \quad (16)$$

The inputs to the model are the parameters (γ_1, γ_2, η_c, η_d, α_c, α_d, $a_1(I)$, $a_2(I)$, $V_{nom,c}$, $V_{nom,d}$), $b(k-1)$, and $p(k)$. The output of the model is the battery energy content $b(k)$. As mentioned, we approximate the functions $\eta_c(I), \eta_d(I)$, $a_1(I)$, and $a_2(I)$ with constants η_c, η_d and lines for a_1, a_2.

4. DETERMINING PARAMETERS

There are two methods to obtain the values for the parameters of our models. The first is from the battery specification sheet (spec) that is published by the manufacturer of the battery being modelled, and the second is to use an IV measurement trace. We use the Leclanché Li-Titanate cell specifications document [11] as an example. This document contains reversible discharge curves, such as the ones shown in Figure 4, as well as the nominal voltage and impedance values. In the spec, charging and discharging rates are often given in terms of current, i.e., C-rate, where 1C is the current at the output of the BMS needed to fully charge or discharge the battery in 1 hour. For the Li-Titanate cell, 1C corresponds to 30 Ampere current.

Unfortunately, the spec may not have all the information needed to derive the model parameters. For example, the reversible discharge curves in Figure 4 only have discharge rates up to 2C even though the spec recommends an upper limit of 4C discharging. Thus, one source of error is due to the interpolation of these curves for higher rates. Moreover, the spec gives the average parameters for the class of Li-Titanate cells, but each cell has slightly different parameters. This is a second source of spec error.

If a measurement trace for the cell, that is, a trace of battery voltage as a function of a sequence of charge/discharge operations, were available, it can be used to obtain model parameters, as discussed next. These parameters are specific to the cell under test and therefore do not exhibit spec errors.

Thus, obtaining model parameters both from the spec and from experimental traces allows us to distinguish between modelling errors and errors due to the spec. In practice, since experimental traces are hard to obtain, our models would exhibit the sum of these errors.

In this section, we discuss how to obtain parameter values using both of these methods. The resulting parameter values for a Li-Titanate cell are presented in Table 5 (Appendix) if they are constants for Model 1, or in Figures 6, 7, and 8 if they are functions.

The parameters for Model 1 and 1* need to be representative and will differ based on the operating range over which the battery is used. To reflect this, in this paper we take the average values in the charging (resp. discharging) operating range as our representative values for those parameters which are constant approximations to a curve. We use the notation 'Model #[x,y]' to mean "Model #, with parameters approximated in the operating range between x and y", where x is the largest (negative) discharging current, and y is the largest charging current in the operating range. Note that the models have some parameters in common (α_c, α_d, η_c, η_d, γ_1, γ_2); the values for these parameters in the same operating range will be identical for each model.

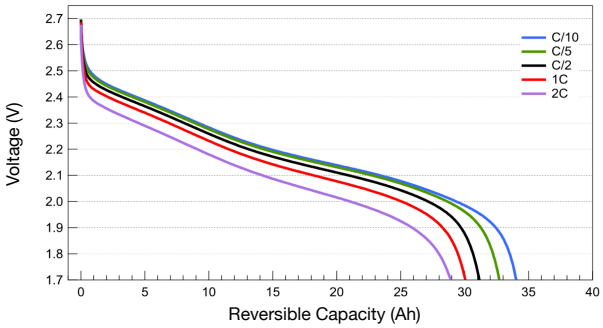

Figure 4: Reversible discharge capacity for different discharge rates from the specification sheet for Li-Titanate [11].

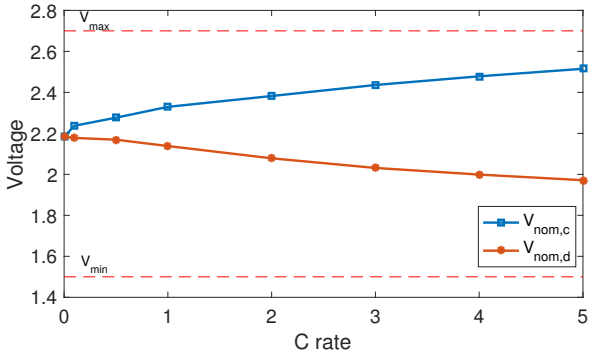

Figure 5: Nominal voltages for a Li-Titanate cell.

4.1 Nominal voltage: $V_{nom,c}$, $V_{nom,d}$

The nominal voltages are parameters for Model 1*. For a given C-rate, we take the nominal voltage to be the average cell voltage during a full charge or discharge. It can be easily derived from a reversible capacity curve from the spec, shown in Figure 4, or from measurements. Figure 5 shows the nominal voltage for each of the measured C-rates. For model 1*[x,y]. $V_{nom,c}$ and $V_{nom,d}$ are calculated as the average of the nominal voltages for the current range [x,0] and [0,y], respectively.

4.2 Energy content limits: a_1, a_2, $a_1(.)$, $a_2(.)$

These parameters represent the lower and upper limits on the energy content. They are constant in Model 1, and depend on the operating range. In Model 1* and Model 2, they are functions of the current. a_1 models the fact that the battery cannot be discharged fully at high discharge currents due to the voltage drop, while a_2 models mirrored effects of the voltage jump when charging the battery.

These functions can be obtained from the voltage vs. re-

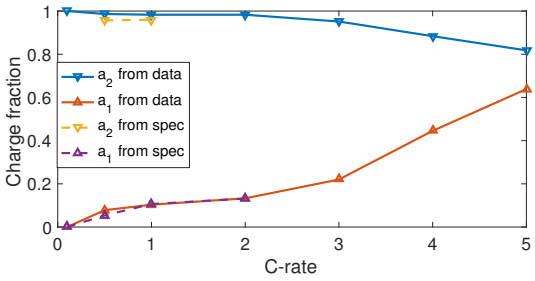

Figure 6: a_1 and a_2 as a function of the current for a Li-Titanate cell. Values derived from the measurements traces as well as the specs are shown. The spec did not show reversible capacity curves for as large a range as the measurement trace.

versible capacity curves such as the ones shown in Figure 4 from the spec, or using similar curves obtained from a measurement trace that cycles the battery using the range of currents the battery is designed to handle. When the battery voltage reaches V_{min} while a high discharge current is applied, it does not mean that there is no energy in the battery; rather, it means that the remaining energy can be accessed only at a lower discharge current. We choose the value of $a_1(I)$ to be the energy remaining in a battery when the voltage reaches V_{min} while being discharged with current I. A similar effect can be seen when charging a battery. We choose the value of $a_2(I)$ to be the energy in the battery when the voltage reaches V_{max} at current I. Figure 6 shows the a_1 and a_2 curves derived from both the spec and measurement traces.

Model 1[x,y] uses the average values for a_1 and a_2 in the given operating range. Model 1*[x,y] uses linear approximations to the a_1 and a_2 curves in the given operating range. In this paper, we use the least-squares linear approximations to the true curves. The curves are a function of the current, which is approximated as $p(k)/V_{nom,d}$ for discharging. The resulting $a_1(p(k)/V_{nom,d})$ for Model 1* is:

$$a_1(\frac{p(k)}{V_{nom,d}}) = m\frac{p(k)}{V_{nom,d}} + i, \tag{17}$$

where m and i are the parameters of the line that approximates the true a_1 curve in the range [x,y]. $a_2(p(k)/V_{nom,c})$ is obtained in similar fashion.

4.3 Voltage function: M

The function M, which maps energy content and current to charging or discharging voltage can be approximated using the reversible capacity curves obtained from either the spec or a measurement trace. The curves map ampere-hour content and current to voltage, and by taking the product of the ampere-hour content and nominal voltage value to get an energy value, we get a good approximation to M. Figure 7 shows the resulting shape of M when derived using the reversible capacity curves from the measurement trace. We use a linear interpolation of the available points as our function M, which maps the energy content in the domain [0Wh,72.5Wh] and current in the domain [-5C, 5C] to voltage in the range [1.5V, 2.7V]. When the specification's reversible capacity curves are used, we get M with energy content in the domain [0Wh, 74.8Wh]current only in the

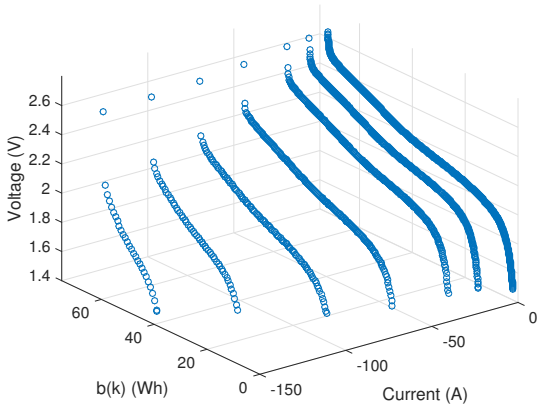

Figure 7: M function for discharging currents, derived using reversible capacity curves from the measurement trace.

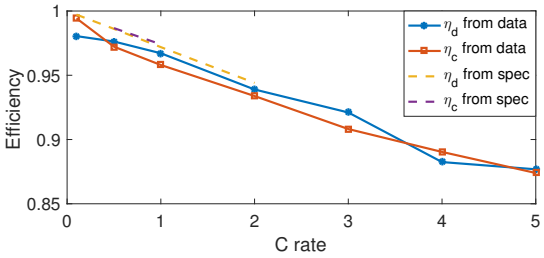

Figure 8: Li-Titanate charging/discharging efficiency as a function of the current, calculated using the impedance value from the spec [11] and compared to what we observe in the measurement traces.

domain [-2C, 1C] and voltage in the range [1.7V, 2.7V]; this limitation effects the range of charging and discharging rates that we can use to validate our model with spec-derived parameters.

4.4 Efficiency: η_c, η_d, $\eta_c(.)$, $\eta_d(.)$

Since η_c and η_d are constant in Model 1[x,y] and 1*[x,y], we set η_c and η_d to be the mean efficiency values in the operating range [x,y].

For Model 2, the efficiency, which we take to be a function of I, can be calculated by using the impedance value R_i (provided by the spec) in the following calculations:

$$\text{efficiency} = \frac{\text{useful power}}{\text{total power}} = \frac{I^2R_L}{I^2(R_L + R_i)}.$$

Substituting $R_L = \frac{V - IR_i}{I}$, we get

$$\text{efficiency} = 1 - \frac{IR_i}{V} \implies \eta_c(I(k)) = 1 - \frac{I(k)R_i}{V(k)} \tag{18}$$

For simplicity, instead of $V(k)$ we use the nominal voltage $V_{nom,I}$ for each charging and discharging current, and hence

$$\eta_c(I(k)) = 1 - \frac{I(k)R_i}{V_{nom,I(k)}} \tag{19}$$

Both charging and discharging efficiency functions can be calculated this way.

A measurement trace can give us the difference between input and output energy in one full cycle, and thus the round-trip efficiency, which is a product of η_c and η_d. We describe how to isolate the efficiency values by fitting the values to what we observe in measured data in Appendix B. Figure 8 shows the resulting efficiency function derived from a measurement trace and the spec, using $R_i = 2$ mOhms.

4.5 Charging/Discharging limits: α_c, α_d

The specifications give recommended maximum charging and discharging C-rates. These are converted into α_c and α_d power limits by taking the product of the C-rate limits and the corresponding nominal voltage of the C-rate. If using a measurement trace to obtain these parameters, α_c is set so that it does not exceed the maximum observed charging power (the same for α_d and discharging power) provided that the battery was tested at its maximum charging and discharging rate when the measurements were taken. In practice, these limits are enforced by the control component of the battery which prevents charging and discharging rates that would cause damage to the battery[2].

4.6 Self-Discharge: γ_1, γ_2

Unfortunately, the self-discharge parameters (γ_1, γ_2) are neither included in the spec nor derivable from our available measurement traces. For Li-ion cells, self-discharge is almost negligible within short-term experiments, making it difficult to validate the effect of self-discharge on our models. The literature suggests that the self-discharge of Li-ion batteries follows a curve that can be modelled with the parameters we use, and is less than 3% of the total capacity per month [18, 21]. In the evaluation of our models, our longest experiment lasts up to 110 hours over which the effects of self-discharge would not be noticeable, so we set both γ_1 and γ_2 to 0.

5. VALIDATION

In this section, we describe the data we used to compare our models with measured results from two Li-Titanate and two LiFePO4 cells. We also describe the metrics for comparison, and present our results in the form of figures and error tables. As discussed earlier, to distinguish between errors caused by parameter estimation and errors inherent to the model, we use parameters both from the spec and from measurements.

5.1 Experimental Data

The measurements were performed for two Li-Titanate and two LiFePO4 energy storage cells under different conditions. The Li-Titanate cells [11] have a voltage range of [1.7,2.7] V, and nominal capacity of 30 Ah, although with low discharging rates a capacity of at least 32.7 Ah is possible. The LiFePO4 cells [1] have a voltage range of [2,3.6]V, and nominal capacity of 1.1 Ah.

We ran a series of lab experiments using BaSyTec XCTS Lab battery testing equipment (manufactured by BaSyTec GmbH, Germany), which has a programmable interface for specifying the charging and discharging processes of a cell, and mimics a battery controller programmed to prevent the battery voltage from going beyond $[V_{min}, V_{max}]$. The equipment gives precise measurements of battery voltage and current. The cells were placed in a Binder MK 53-E2 climate control chamber (Binder GmbH, Germany) during testing.

The experiments that we conducted test the limits of each single-cell battery in terms of both voltage and current by cycling the cell under different currents and recording the current, voltage, and total charge (Ah) every 10 seconds. We also ran experiments using a variable charging and discharging profile that reflects how a battery would be used to provide back-up power in a system with a solar power source and building load over an 8-hour period, with a measurement granularity of 1 second.

In the experiments with the Li-Titanate cell, we allowed the voltage to drop to 1.5 V, which is lower than the recommended minimum of 1.7 V given by the spec. We were still able to obtain parameter values for our model by using the measurement trace that contains the low voltages. We could not use the spec to obtain parameters to model this behaviour, and therefore limit the comparison of our model with spec parameters to the measured data when the voltage lies in the permissible range.

5.2 State of Charge Metric

We evaluate our models by comparing the state of charge (SoC) of the test cells with the SoC computed by each model. We define the SoC of a battery at current I to be the usable energy in the battery divided by the total capacity at that current. This metric allows us to determine both how accurately our models calculate the energy content as well as how close our models are to limiting the battery to the acceptable voltage range without actually estimating the voltage. Specifically, the SoC in time slot k is calculated as

$$SoC(k) = \frac{b(k) - a_1(I(k))}{(a_2(I(k)) - a_1(I(k)))} \tag{20}$$

The SoC of a test cell as it is being charged or discharged can be inferred by using a set of mappings from measured voltage to SoC. V_{min} is mapped to an SoC of 0, V_{max} is mapped to an SoC of 1, and the measured charge of the battery is used to calculate SoC as the battery is cycled. In this way, we obtain the SoC of each measured cell using the measurement traces of each cell. Figure 9 shows a sample of the mappings we used to infer the SoC of one of the measured cells. This SoC is compared with the SoC suggested by simulating our models using the same charging and discharging processes.[3]

5.3 Evaluation

To evaluate our models, we used two Li-Titanate cells and two LiFePO4 cells, and cycled them using each cell's range of recommended charge and discharge currents. We then simulated one of our models using the same charging and discharging current that were used in our lab experiments, and compared the SoC of the modelled and real single-cell battery. The inputs $b(k-1)$ and $V(k-1)$ were initialized to be the observed value in the first time step of the simulation, and each subsequent time step used the modelled values of the previous time step as input, which can potentially cause an accumulation of errors. Each case study differs in (a)

[2]In the measurement trace we used, the control component was bypassed which allowed us to test currents that are beyond the range recommended by the spec.

[3]The exception to this is when our modelled cell would have been overcharged or undercharged using the power values from the measurement traces, in which case we clip the power to prevent this from happening.

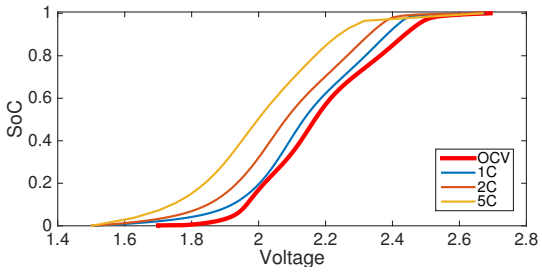

Figure 9: Experimentally-derived Voltage-SoC mapping for a Li-Titanate cell discharged at various C-rates, as well as at Open Cell condition (OCV).

the model we simulate, (b) how we derived the parameters, (c) the cell chemistry, and (d) the type of charging and discharging that we test. We calculated the average residual at each C-rate separately, to give a sense of the range where the models perform well and where they do not.

Due to limitations of space, although we studied significantly more, we can only describe eight case studies in Table 2, and present the results in Table 3 by showing the mean residual between measured and modelled SoC, averaged from the two cells of the technology being used in the case study. In each of the case studies, we compare the measured and modelled energy content for each charging and discharging current, which lasts 2-3 cycles. This is done to isolate the errors at each charging/discharging rate being tested. Case studies E0-E7 look at how variations in the discharging current affect the modelling of Li-Titanate cells, whose a_1 bound changes significantly with the discharge current, and the corresponding errors in Table 3 are for discharging C-rates. Case study E8 looks at how variations in the charging current affect the modelling accuracy of the LiFePO4 cells, whose a_2 bound changes significantly with the charge current, so the errors for E8 in Table 3 are given for charging C-rates.

Figure 10 shows the results of case studies E1 and E3. For clarity, we choose to represent the rest of our results in terms of the residual, which is the absolute difference between SoC observed in the real cell and the modelled SoC. We show the residuals from one of the cells in each of the eight case studies in Table 4. In these figures, E0-E7 show SoC residual during discharging, while E8 shows SoC residual during charging. Residual figures for E1 and E4 feature a dashed line showing the extent of the operating range over which the parameters were calibrated in those case studies.

We comment on each case study below.

E0: Model 1 is not accurate for the full operating range [-5C, 5C]. The best accuracy occurs at 3C discharging because the η_d and a_1 parameter values (chosen as the average values of their respective functions in the operating range) are close to the real values at 3C.

E1: The performance of Model 1 at charge/discharge rates below 1C, with parameters that are calibrated for low charging and discharging rates [-1C, 1C], is good.

E2: Model 2 significantly lowers the residual at high discharge rates with respect to Model 1. The highest residual occurs at the first 5C discharge cycle. Upon inspection, it was determined that the voltage during this cycle behaves very differently from what we observe during the two other 5C cycles in the experiment. See Section 6 for more details.

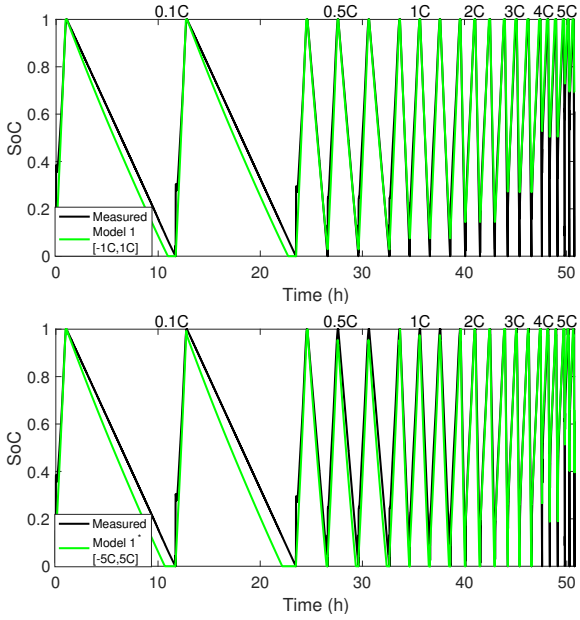

Figure 10: Comparison of measured SoC with modelled SoC.

E3: Model 1* shows a significant improvement over Model 1 for higher discharge rates. The a_1 parameter here is a linear approximation to the curve used in Model 2 (Figure 6), while the efficiency parameters are chosen to be the average over the entire range of charging and discharging. The linear approximations happen to be a poor match to the a_1 values at 2C, 3C, and 5C discharging, which is why the model is less accurate for these C-rates.

E4: When we restrict the upper limit of discharging currents to 3C rather than 5C when doing a linear fit to the a_1 function and calibrating the efficiency, the accuracy of Model 1* improves significantly for discharging currents up to 3C. This is expected, since approximating over a smaller range should result in parameters that are closer to the values in that range.

E5-E7: The spec is slightly worse than measured parameters at describing cell behaviour for all models. The biggest difference in accuracy is seen with Model 1*. This is because the a_2 function derived from the spec for Li-Titanate is not a good match of what we observe in the measurements (see Figure 6). This parameter error throws off the accuracy of the charging portion of the experiment and carries over into the errors observed during discharging.

E8: Model 1* performs exceptionally well for varying charge curves. This is due to the linear shape of the a_1 and a_2 functions derived from the LiFePO4 cells.

Additional Case Studies:

- When using Model 1 to model a LiFePO4 cell, the average SoC error was less than 3.5% for charging rates

up to 3C and discharging rates up to 5C. Thus Model 1 appears to be an adequate model for this technology up to 3C charging and 5C discharging. The error grew to 7% at 4C charging and 10C discharging, which is allowed by the specification. The accuracy with Model 2 and Model 1* was outstanding for this cell type (< 5% error for all tested rates).

- We also tested a more realistic charge discharge behaviour with charging from a solar trace and discharge from a building load. In this test, we found ≈ 3% SoC residual for all models, with Model 2 slightly outperforming Model 1*, and Model 1* slightly outperforming Model 1. We find these small discrepancies are due to the fact that the charging and discharging rates in this experiment are no higher than 1C.

6. DISCUSSION

6.1 Insights

Our cases studies have given us insights into where our models perform well and where they do not.

Model 1 is error-prone when the charging and discharging rate significantly impact the usable capacity of the battery but can perform well if the operating range, i.e., the range of charging and discharging rates, of the battery being modelled is narrow. With Model 1, parameters should be chosen to match the middle of the operating range in order to reduce the average error. Given the limitation of Model 1, determining if existing work that uses this model is invalidated is not a straightforward task, since the storage technology being modelled is not always specified. If the cell technology is Li-ion, it is also necessary to know the cell chemistry, which, as our experiments have shown, has a significant role on the accuracy of Model 1.

With Model 2, the largest inaccuracies are observed when the voltage changes rapidly, often seen when the battery is nearly full or nearly empty. If our energy content calculation is even 1-2% off, it can cause a domino effect that affects the estimate of the voltage, which then affects the estimate of the current, which affects the value of a_1 and a_2 functions; this problem is exacerbated if the voltage changes significantly. However, the usable capacity of the battery is not just limited by its voltage limits, but also by the controller in order to preserve the increase in lifetime of the battery [16]. This widely recommended approach to battery management would limit the voltage to a range that is narrower than $[V_{min}, V_{max}]$ where it does not jump or drop significantly, i.e., a range where Model 2 has demonstrated exceptional accuracy.

Model 1* performs well when the a_1 and a_2 functions are roughly linear with respect to the current. As seen in our comparison of results from E3 and E4, Model 1* performs better when the operating range is slightly narrowed, so that the linear approximation is accurate, and all our case studies show us that Model 1* has low errors over a much wider operating range than Model 1.

We observed that the spec parameters did not reflect battery performance as well as the measured parameters, which was an expected result. However, in a battery with many cells, individual differences seen in cells should average out, making the spec more accurate. Thus, the *battery* errors would likely be smaller than *cell* errors; verifying this insight is part of our future work.

6.2 Model 1* parameter approximations

Model 1 and Model 2 represent two points on an accuracy-tractability spectrum, with Model 1* occupying a middle point on this spectrum, because it is more accurate than Model 1 but more tractable than Model 2, making it more useful for a researcher who wishes to integrate a storage model into an optimization framework. It is possible to employ different approximations than those we used to obtain a different version of Model 1*. We discuss our choices next.

6.2.1 Voltage Approximation

In Model 2, a voltage estimate is an internal parameter used to estimate $I(k)$, which is the input to the η_d, η_c, a_1, and a_2 functions. While this model is suitable for simulation, the requirement for iterative computation of $V(k)^*$ makes it difficult to integrate it into an optimization framework. In Model 1*, we use one of the two appropriate nominal voltages, one for charging and one for discharging of the cell, to be the voltage estimates.

6.2.2 Energy Limit Approximation

The a_1 and a_2 functions in Model 2 are derived from the reversible capacity curves, which we use to get a collection of points whose interpolation defines the function. To be useful in an optimization problem, we would need an analytical approximation to the function. In Model 1*, we decided to use linear approximations because they gave an acceptable approximation to the set of points.

6.2.3 Efficiency Approximation

A primary contributor to the complexity of Model 2 is the multiplication of the efficiency functions by the input power. In many optimization models, the operation of the battery, i.e., the charging/discharging power, is a variable. The multiplication of the power by the efficiency, which is a function of the input power, creates a non-linear constraint. To keep the constraint linear, Model 1* uses constant η_d and η_c values. We could use a linear approximation for the efficiency, as suggested by Figure 8, if the improved accuracy is worth sacrificing the linearity of the model.

6.3 Limitations

Although our models demonstrate a trade off between fidelity and complexity, we are aware that they are far from perfect. We do not take into account several factors that may influence the behaviour of a Li-ion battery, such as state of health and temperature effects which are known to limit the available capacity of the battery [3, 19]. We do not model the internal state of the battery in any detail, which means that we may be missing the opportunity to model some key behaviours that would improve the accuracy without sacrificing the simplicity of our models. We have not studied the scaling behaviour of our models for multi-cell batteries; this is future work.

7. CONCLUSIONS

Any model for Li-ion storage must make a tradeoff between accuracy and tractability, when used as part of an optimization problem. We have evaluated three different models that make different trade-offs. We find that a model

Table 2: Description of Case Studies

Case Study	Model	Parameter Source	Cell Chemistry	Description
E0	1[-5C,5C]	Measured	Li-Titanate	Cell is charged at 1C and discharged at a constant rate between 0.1 and 5C in each cycle.
E1	1[-1C,1C]	Measured	Li-Titanate	“”
E2	2	Measured	Li-Titanate	“”
E3	1*[-5C,5C]	Measured	Li-Titanate	“”
E4	1*[-3C,3C]	Measured	Li-Titanate	“”
E5	1[-2C,1C]	Spec	Li-Titanate	Cell is charged at 1C and discharged at a constant rate between 0.1 and 2C in each cycle.
E6	2	Spec	Li-Titanate	“”
E7	1*[-2C,1C]	Spec	Li-Titanate	“”
E8	1*[-10C,4C]	Measured	LiFePO4	Cell is discharged at 1C and charged at a constant rate between 0.5 and 4C in each cycle.

Table 3: Average Residual SoC (%).

Case Study	0.1C	0.5C	1C	2C	3C	4C	5C
E0	17.7	14.3	12.9	9.3	1.7	16.5	32.0
E1	5.4	1.2	1.8	5.2	12.3	25.9	38.0
E2	3.0	3.5	4.1	4.0	4.8	7.5	7.0
E3	6.9	7.6	8.1	9.7	9.4	7.0	15.8
E4	4.9	3.7	3.0	2.7	3.4	15.2	28.0
E5	4.2	1.3	2.6	6.4	-	-	-
E6	2.3	2.2	3.7	3.6	-	-	-
E7	3.1	2.4	2.8	3.2	-	-	-
E8	-	0.8	0.9	0.5	1.1	1.1	-

Table 4: State of Charge Residual Figures

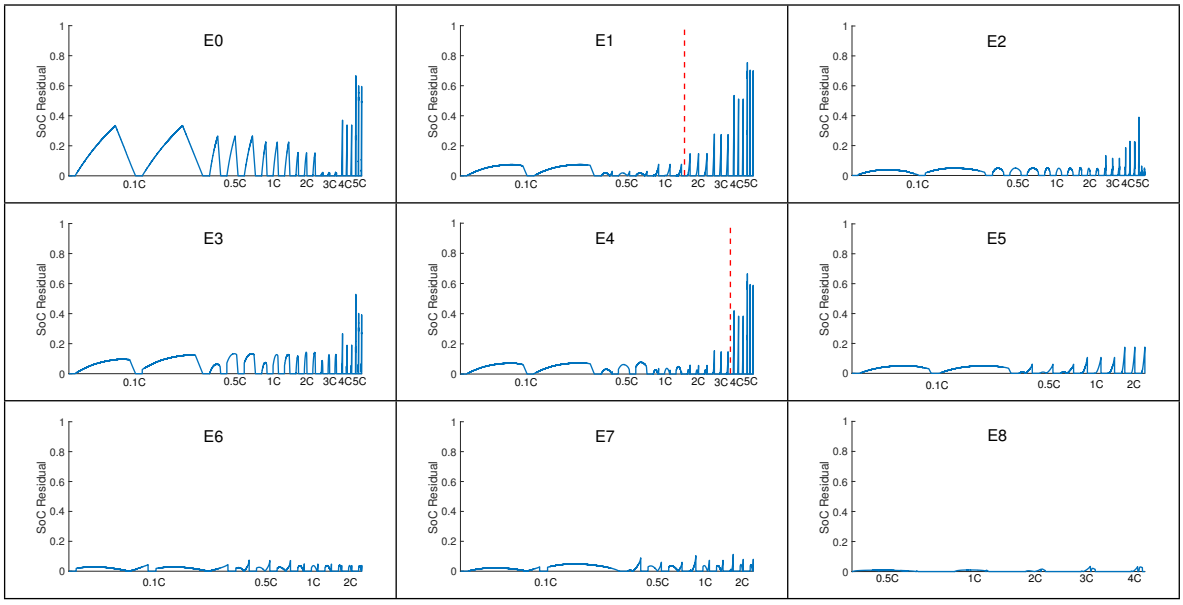

that is commonly used in optimization problems to model storage systems (Model 1) is too simple to accurately model the state of charge of a battery over a wide operating range. Instead we presented a new model (Model 2) that is accurate over a much wider operating range, but is difficult to incorporate into an optimization problem. We then approximate parts of Model 2 to get Model 1*, which is simple enough to be incorporated into an optimization framework while being accurate over a significantly wider operating range compared to Model 1. We believe that our Model 1* is a good balance between accuracy and tractability, and is suitable for use in a variety of optimization problems involving energy systems.

In future work, we plan to compare cell error and battery error when using spec parameters, and to use Model 1* for solving a variety of optimization problems. We also would like to better model the state of health of the battery, as fundamental knowledge about this issue is gleaned.

8. REFERENCES

[1] A123 Systems. *High Power Lithium Ion APR18650M1A*, 2009. LiFePO4 cell specifications.

[2] K. M. Chandy, S. H. Low, U. Topcu, and H. Xu. A simple optimal power flow model with energy storage. In *Decision and Control (CDC), 2010 49th IEEE Conference on*, pages 1051–1057. IEEE, 2010.

[3] D. Doerffel and S. A. Sharkh. A critical review of using the Peukert equation for determining the remaining capacity of Lead-acid and Lithium-ion batteries. *Journal of Power Sources*, 155(2):395–400, 2006.

[4] N. Gast, J.-Y. Le Boudec, A. Proutière, and D.-C. Tomozei. Impact of storage on the efficiency and prices in real-time electricity markets. In *Proceedings of the fourth international conference on Future energy systems*, pages 15–26. ACM, 2013.

[5] Y. Ghiassi-Farrokhfal, F. Kazhamiaka, C. Rosenberg, and S. Keshav. Optimal design of solar PV farms with storage. *Sustainable Energy, IEEE Transactions on*, 6(4):1586–1593, 2015.

[6] Y. Ghiassi-Farrokhfal, S. Keshav, and C. Rosenberg. Toward a realistic performance analysis of storage systems in smart grids. *Smart Grid, IEEE Transactions on*, 6(1):402–410, 2015.

[7] H. He, R. Xiong, and J. Fan. Evaluation of Lithium-ion battery equivalent circuit models for state of charge estimation by an experimental approach. *Energies*, 4(4):582–598, 2011.

[8] X. Hu, S. Li, and H. Peng. A comparative study of equivalent circuit models for Li-ion batteries. *Journal of Power Sources*, 198:359–367, 2012.

[9] R. Huang, S. H. Low, U. Topcu, K. M. Chandy, and C. R. Clarke. Optimal design of hybrid energy system with PV/wind turbine/storage: A case study. In *Smart Grid Communications (SmartGridComm), 2011 IEEE International Conference on*, pages 511–516. IEEE, 2011.

[10] F. Kazhamiaka, C. Rosenberg, and S. Keshav. Practical strategies for storage operation in energy systems: design and evaluation. *Accepted to IEEE Transactions on Sustainable Energy*, 2016.

[11] Leclanché. *LecCell 30Ah High Energy*, 02 2014. Lithium-Titanate cell specifications.

[12] A. Mishra, R. Sitaraman, D. Irwin, T. Zhu, P. Shenoy, B. Dalvi, and S. Lee. Integrating energy storage in electricity distribution networks. In *Proceedings of the 2015 ACM Sixth International Conference on Future Energy Systems*, pages 37–46. ACM, 2015.

[13] B. Nykvist and M. Nilsson. Rapidly falling costs of battery packs for electric vehicles. *Nature Climate Change*, 5(4):329–332, 2015.

[14] N. Omar, P. V. d. Bossche, T. Coosemans, and J. V. Mierlo. Peukert revisited – critical appraisal and need for modification for Lithium-ion batteries. *Energies*, 6(11):5625–5641, 2013.

[15] J. Qin, Y. Chow, J. Yang, and R. Rajagopal. Modeling and online control of generalized energy storage networks. In *Proceedings of the 5th international conference on Future energy systems*, pages 27–38. ACM, 2014.

[16] P. Ramadass, B. Haran, P. M. Gomadam, R. White, and B. N. Popov. Development of first principles capacity fade model for Li-ion cells. *Journal of The Electrochemical Society*, 151(2):A196–A203, 2004.

[17] K. A. Smith, C. D. Rahn, and C.-Y. Wang. Control oriented 1d electrochemical model of Lithium ion battery. *Energy Conversion and Management*, 48(9):2565–2578, 2007.

[18] M. Swierczynski, D.-I. Stroe, A.-I. Stan, R. Teodorescu, and S. K. Kaer. Investigation on the self-discharge of the lifepo4/c nanophosphate battery chemistry at different conditions. In *Transportation Electrification Asia-Pacific (ITEC Asia-Pacific), 2014 IEEE Conference and Expo*, pages 1–6. IEEE, 2014.

[19] J. Vetter, P. Novák, M. Wagner, C. Veit, K.-C. Möller, J. Besenhard, M. Winter, M. Wohlfahrt-Mehrens, C. Vogler, and A. Hammouche. Ageing mechanisms in Lithium-ion batteries. *Journal of power sources*, 147(1):269–281, 2005.

[20] S. S. Zhang. The effect of the charging protocol on the cycle life of a Li-ion battery. *Journal of power sources*, 161(2):1385–1391, 2006.

[21] A. H. Zimmerman. Self-discharge losses in lithium-ion cells. *Aerospace and Electronic Systems Magazine, IEEE*, 19(2):19–24, 2004.

APPENDIX

A. PARAMETER TABLE

Table 5: Model 1[-1C,1C] Li-Titanate parameter values from specifications and measurements.

Parameter	Spec	Measured
a_1	4 Wh	3.9 Wh
a_2	74 Wh	71.9 Wh
α_c	4C	5C
α_d	4C	5C
η_c	0.981	0.975
η_d	0.974	0.967
γ_1, γ_2	N/A	N/A

B. CALCULATING EFFICIENCY FROM MEASUREMENT TRACE

A measurement trace can be used to calculate the difference between input and output energy in one full cycle, giving us the round-trip efficiency which is a product of η_c and η_d. To separate the values, we make two assumptions and using the characteristics of our trace to isolate the efficiencies at different C-rates. We make the following assumptions:

1. The charging efficiency at 1C is some value X.
2. The amount of energy that is used to charge the battery after efficiency losses are accounted for is equal to the amount of energy discharged from the battery (including the losses due to efficiency).

The first assumption gives us a starting point from which to calculate the rest of the efficiency values, and is a guess for the true efficiency at 1C. A good guess for Li-Titanate could be $X = 0.97$, which is the efficiency value given by Eq. 19 at 1C, although we found that $X \approx 0.96$ better reflects what we observe in the trace.

For assumption 2 to hold, the energy content of the battery should be the same for when the cycle starts (first charging step) and when it ends (last discharging step), which holds if the preceding cycle was charged/discharged using the same currents. Assumption 2 can be expressed using the following equation:

$$\eta_c \cdot TotalChargingEnergy = \frac{TotalDischargingEnergy}{\eta_d} \tag{21}$$

This equation can be rearranged to isolate η_c or η_d.

The measurement trace be used to calculate the total discharging and charging energy, but we are left with two unknowns (η_c, η_d). These could be isolated by using a particular measurment trace in combination with assumption one. We require a trace that keeps the charging rate constant at 1C, and varies the discharging rate. By fixing a value for η_c at 1C via assumption 1, we can use Eq. 21 to get the discharging efficiencies for discharge rates that cover the full operating range of the battery. We then use a second trace where the charging rate varies and discharging is always at a constant rate. We use Eq. 21 and the newly calculated η_d values to isolate the charging efficiency for charging rates of the full operating range. The values we obtain through this approach end up being very close to the values obtained from the spec, suggesting that the spec is enough to get a good estimate of the efficiency functions.